Femtosecond Real-Time Probing of Reactions. 13. Multiphoton Dynamics of IHgI

S. Pedersen, T. Baumert,[†] and A. H. Zewail*

Arthur Amos Noyes Laboratory of Chemical Physics,[‡] California Institute of Technology, Pasadena, California 91125

Received: September 9, 1993[⊛]

Real-time studies of the dynamics were performed on the reaction of HgI_2 in a molecular beam. Excitation was by either one or multi pump photons (311 nm), leading to two separate sets of dynamics, each of which could be investigated by a time-delayed probe laser (622 nm) that ionized the parent molecule and the fragments by REMPI processes. These dynamics were distinguished by combining the information from transients taken at each mass (HgI_2, HgI, I_2, Hg, and I) with the results of pump (and probe) power dependence studies on each mass. A method of plotting the slope of the intensity dependence against the pump–probe time delay proved essential. In the preceding publication, we detailed the dynamics of the reaction initiated by a one photon excitation to the A-continuum. Here, we present studies of higher-energy states. Multiphoton excitation accesses predissociative states of HgI_2, for which there are crossings into the symmetric and asymmetric stretch coordinates. The dynamics of these channels, which lead to atomic (I or Hg) and diatomic (HgI) fragments, are discussed and related to the nature of the intermediates along the reaction pathway.

I. Introduction

For the reaction of HgI_2, the dynamics were probed in earlier studies using laser-induced fluorescence (LIF) on the femtosecond time scale.[1-4] At a fixed probe wavelength (390 or 620 nm), the fluorescence of HgI, monitored at different wavelengths, was recorded at different delay times. Dispersion of the fluorescence spectrum[5,6] allowed for separation of the different set of trajectories which produce coherence in the final products. There are three coordinates involved in the IHgI reaction, one symmetric stretch, one asymmetric stretch, and one bend, and the molecular dynamics simulations[2,3] revealed the wave packet motion in these coordinates, making comparison with experiments.

In the preceding publication,[7] we reported on the use of the kinetic energy time-of-flight (KETOF) technique in the femtosecond time-resolved study of IHgI fragmentation. With this technique, we were able to measure the scalar part (kinetic energy release) as well as the vectorial part (symmetry and alignment of transition moments) of the dynamics while the system is in the transition-state region. The emphasis was mainly on the early time (up to about 500 fs) behavior, and as will be shown here, this behavior corresponds to one-photon excitation to the A-continuum.

In this paper, mass selectivity is employed in determining the dynamics involved in one- and multi-pump-photon excitation of IHgI. The parent mass (HgI_2^+) and each of the four fragment masses (HgI^+, I_2^+, Hg^+, and I^+) were monitored during the course of the reaction and when final fragments were formed. Pump and probe intensity studies were analyzed with a very simple method, distinguishing and identifying the temporal behavior of the dynamics in the one-photon and multiphoton regimes.

The outline of the paper is as follows: in section II a brief description of the experiment is given. The results are presented in section III and include an analysis of the pump and probe power dependence studies. The discussions are given in section IV, and the summary and conclusions follow in section V.

II. Experimental Section

The femtosecond laser apparatus has been described in detail previously[8] and is discussed only briefly here. Femtosecond pulses were generated from a colliding pulse mode-locked ring dye laser (CPM) and amplified by a Nd:YAG-pumped pulsed dye amplifier (PDA). The recompressed output pulses had an (unattenuated) energy of 0.2–0.3 mJ at a repetition rate of 20 Hz. The pump wavelength was 311 nm (fwhm = 5 nm) and was generated by frequency doubling a part of the PDA output in a 0.2-mm-thick KDP crystal. For the probe MPI we used the remaining output of the PDA (622 nm, fwhm = 13 nm).

The pump and probe beams, with proper attenuation and parallel or perpendicular polarization, were delayed in time relative to one another in a Michelson interferometer and were then recombined collinearly and focused onto the IHgI molecular beam. The temporal pulse characterization was performed following the procedure of ref 7: the probe was found to have a fwhm of 60 fs ($sech^2$ fitting), and the pump–probe Gaussian cross correlation had a fwhm of 100 fs.

The molecular beam consisted of an oven with a nozzle diameter of 0.3 mm. The oven was heated to 445 K (measured at the nozzle). MPI pump–probe experiments on the skimmed molecular beam were carried out in a differentially-pumped ionization chamber about 12 cm downstream from the nozzle. The TOF spectrometer was used in its mass-resolution mode; the results obtained using its kinetic energy resolution mode were described in ref 7. The molecular beam, the lasers, and the TOF detection axes were mutually perpendicular. In all experiments described here, the pump laser polarization was kept fixed and parallel to the TOF axis. A sketch of the experimental setup is shown in ref 7.

Pump and probe power dependences were performed on all five masses: HgI_2, HgI, I_2, I, and Hg. For these, the probe polarization was maintained fixed perpendicular to the pump polarization. The intensity of one arm, set using a variable attenuator mounted on a translation stage, was monitored after passing through the molecular beam using a photodiode and appropriate filters to exclude the second wavelength. Meanwhile, the other arm was kept at an intermediate level of intensity. After a set of transients were taken at five different intensities of one arm, the variable attenuator in that arm was repositioned in its original place to confirm laser stability. The MPI background HgI_2 ion signal due to the pump only was reduced to a negligible level (<5% of the maximum signal in the HgI_2 transient at the maximum pump intensity used in the pump intensity dependence).
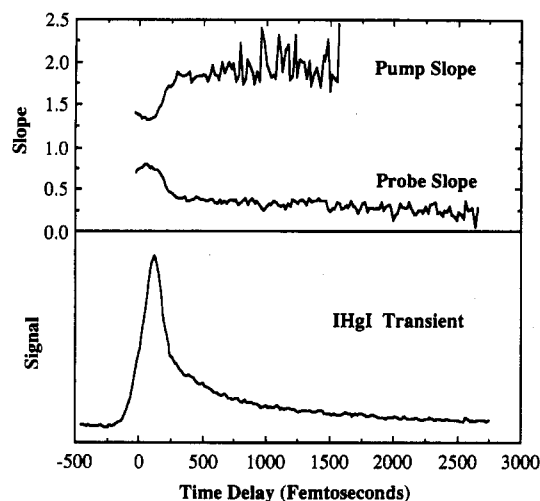
Figure 1. (bottom) The femtosecond HgI_2 transient which shows the multiexponential decay behavior. This transient defines time zero (very close to where the signal has reached half of its maximum value). For this and the other transients shown, excitation is with $\lambda_1 = 311$ nm, and probing is by $\lambda_2 = 622$ nm. (top) The slope of the pump intensity dependence rises from 1.3 ● 0.1 to a constant level of 1.9 ± 0.2 in 200 fs. There is an increasingly stronger probe saturation at long times (slope ~0.4 at 300 fs and 0.25 ± 0.1 at 2.5 ps). Notice that the probe dependence slope mirrors that for the pump (*i.e.*, inverted image) and that there is a temporal correlation between the slope plots and the transient.

Time zero was defined by the position where the HgI_2 signal reached half of its maximum value. In order to find the position of the signal onset in the transients for each mass relative to time zero, scans over a short pump–probe time delay range were taken, alternating between HgI_2 and one of the other four masses. These time zero shift studies were performed with the probe polarization perpendicular to the pump polarization. For each transient, a boxcar gate was set to the mass under investigation and the pump–probe delay line was scanned until a satisfactory signal-to-noise level was achieved.

The sample was 99.999% HgI_2 (Aldrich) containing the natural isotope distribution of Hg (196–204 amu).

III. Results

A. Parent and Fragment Femtosecond Transients.
In Figures 1–5, transients are shown for HgI_2, HgI, I, Hg, and I_2, respectively, for perpendicular polarization of the pump and probe lasers. The time zero shifts are 47 fs for HgI, 61 fs for I, 75 fs for Hg, and 34 fs for I_2. (For each time shift, the uncertainty is ±15 fs.) Hence, each transient has a signal onset that lies later than that of the parent. If the excited wave packet takes some finite time to evolve from the initial region, where probing gives only HgI_2 signal, into a region where a particular fragment mass is obtained upon probing, then this finite time will appear in the time zero shift for the transient of that fragment mass. The time shift is unaffected by the pump or probe intensities if these lie in the unsaturated regime. However, if either the pump or the probe intensity enters the saturation regime, then the onset of the signal will move to earlier times as the intensity is increased. For the HgI_2 transient, the pump is unsaturated and the probe is only weakly saturated. The power dependence for all the other masses is described in the sections that follow.

The HgI_2 transient showed a multiexponential decay behavior. The transient was analyzed as a triple exponential with decay times τ_1, τ_2, and τ_3. To get τ_1, convolution with the pump–probe cross-correlation was required, and a value on the order of 50 fs was obtained. The second component was also fit in the convolution. The third component was most easily obtained from a log plot at long times, yielding a value for τ_3 of about 1 ps. Having determined τ_3, the contribution from this third component
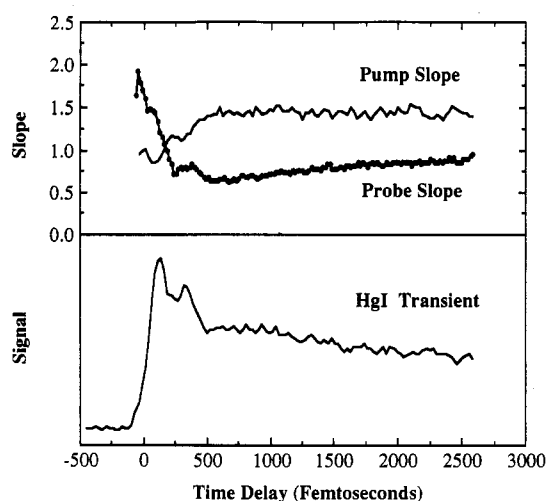

Figure 2. (bottom) The femtosecond HgI transient. Two sharp peaks separated by 220 fs are followed by a broad peak at about 1 ps and by a nonzero asymptote. (top) The pump slope increases from 0.95 ± 0.1 to a constant value of 1.45 ● 0.1 at 500 fs. In the rising part of the pump slope there is a noticeable dip at the position of the second peak in the transient. The probe dependence mirrors the pump dependence: it drops from a slope of more than 1 to a minimum at 500 fs of 0.6 ± 0.1 (some saturation) but then rises again toward 1.
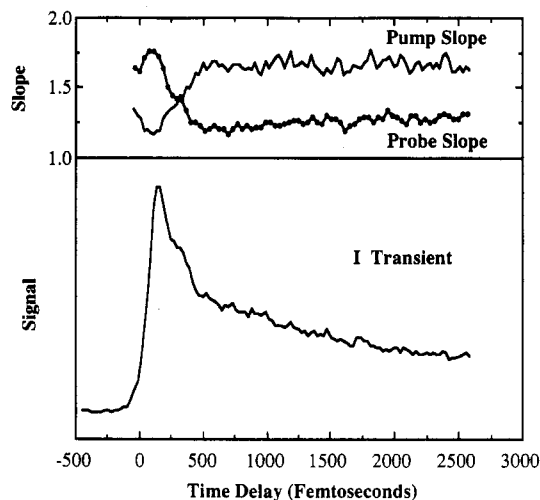

Figure 3. (bottom) The femtosecond transient obtained by detecting the I mass. (top) The slope of the pump intensity dependence rises from 1.3 ± 0.1 to 1.65 ± 0.1 at 500 fs. The slope of the probe intensity dependence shows a mirror image (inverted), decreasing from 1.7 ± 0.1 to below 1.25 (followed by a slight increase again over a picosecond time scale).

($c \exp(-t/\tau_3)$, where c is a constant) was subtracted from the transient, and a log plot of the remainder ($a \exp(-t/\tau_1) + b \exp(-t/\tau_2)$) yielded a value for τ_2 where a linear fit was performed at times much longer than τ_1. Hence, τ_2 was arrived at in two different ways, and in both cases it was found to be on the order of 500 fs.

The I_2 transient (Figure 5) resembles the HgI_2 transient (Figure 1); the signal drops to zero on a time scale of picoseconds, showing that there is no detectable signal from free I_2. The short-time behavior (up to about 500 fs) of HgI, I, and Hg was discussed in detail in ref 7. The emphasis here is on the long-time behavior. In the HgI transient there is an increase (bump) in the signal that is noticeable after 500 fs and peaks around 1 ps (Figure 2). The signal levels off to a nonzero constant value, remaining at this value up to 100 ps (time range checked in the experiment) (Figure 6). The I transient shows a leveling off of the signal after several picoseconds, and as for HgI, this level remains constant up to 100 ps (Figure 6). This asymptotic constant value is, of course, both pump and probe intensity dependent. The Hg transient has a long-time behavior that deviates from that of HgI and I: the
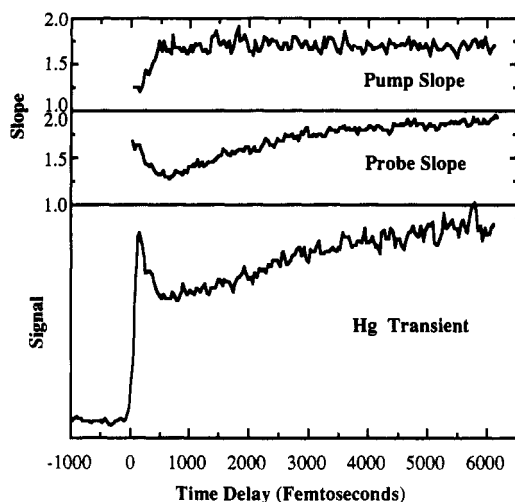
Figure 4. (bottom) The femtosecond transient obtained by detecting the Hg mass (all isotopes). (top) The pump dependence starts off with a slope of 1.25 ± 0.1 up to 100 fs and then rises, reaching an asymptotic value of 1.7 ± 0.1 at 500 fs. The probe dependence slope is initially 1.65 ± 0.1, decreases to a minimum of 1.3 ± 0.1 at 500 fs, and subsequently rises to almost 2 at 2.5 ps.
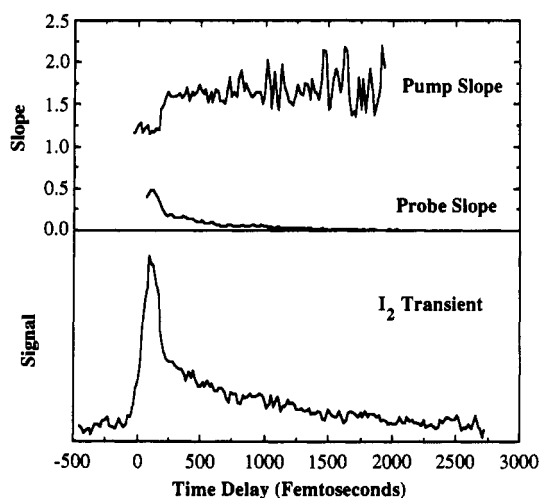

Figure 5. (bottom) The I_2 femtosecond transient which resembles that of HgI_2. (top) The slope of the pump intensity dependence is 1.2 ± 0.1 up to 100 fs, the position of the peak in the transient. The slope then rises in less than 100 fs to an asymptote of 1.65 ± 0.2. The probe slope mirrors the pump slope. There is severe probe saturation after 200 fs.

signal rises at long times, over a range that is on the order of 10 ps (Figures 4 and 6).

The effects of polarization of the pump and probe at early times were described in ref 7. For every mass it was found that at long times there is no significant difference between the transients obtained when the probe was parallel to the pump or perpendicular to the pump. (Note that the pump was always polarized parallel to the TOF axis of the molecular beam and that it was only the probe polarization that was rotated.)

B. Power Dependences. To extract the maximum amount of information from the pump or probe intensity dependence on the transient of each mass, the slope of the power dependence was calculated at each position of the pump–probe time delay. For each value of the time delay, a linear least-squares fit to a graph of ln(signal) *vs* ln(intensity), with data points corresponding to five different laser intensities, was employed to compute the slope corresponding to that time delay. Using this analysis, the slopes of both the pump and probe power dependences could be plotted as a function of the pump–probe time delay, thus tracking and distinguishing between one-photon or multiphoton excitations, the onset of saturation, and the time scales associated with the different processes. Plots of the slopes of the pump and probe
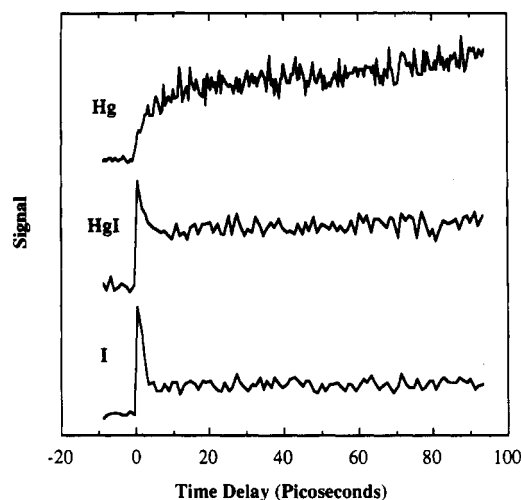

Figure 6. Long-time (up to 100 ps) transients of Hg, HgI, and I. The HgI and I transients show very similar behavior at long times: both have an asymptotic constant signal level (time range limit of experiment). The Hg transient, however, shows a continuous increase in the signal level over tens of picoseconds. Due to the choice of large separation between the data points, the behavior at early times is not well resolved in these transients.

intensity dependences are shown together with the transients for each of the five masses in Figures 1–5. It should be remembered that a slope of less than 1 indicates that a saturated transition contributing to the signal is present. A slope that exceeds 1, having accounted for experimental error, implies that a transition involving more than one photon is present. (Relatively long-lived intermediates may lead to an apparent slope of one, even for a two-photon transition.)

1. Pump Power Dependence. For each mass, five transients were taken over a 1 order of magnitude variation in the pump intensity, keeping the probe fixed. The slope of the intensity dependence was calculated for all values of the pump–probe time delay. The slope plot for every mass is shown together with a transient for that mass. The pump power dependence of the signal can thus be traced as the system evolves. The slope dependence was also performed separately using just the peak values from the five different intensity transients. In the case of HgI_2, for example, this yielded a straight line fit to a plot of ln(signal) *vs* ln(intensity) with a slope of 1.33, consistent with the slope plot value.

The transients for the five different masses show some common features. At early times, in a range up to about 100 fs beyond time zero, the slope of the pump intensity dependence is approximately equal to 1, and then the slope rises to a constant asymptotic value that lies in the range 1.8 ± 0.3. The time taken for the slope to rise is not the same for all five masses. HgI, Hg, and I each have a rise time of about 400 fs; HgI_2 has a slope that rises over a range of 200 fs, while I_2 reaches its asymptotic slope value with a rise time of 100 fs.

2. Probe Power Dependence. The probe intensity was varied in five increments over 1 order of magnitude. The slope of the probe dependence was calculated as a function of the pump–probe time delay for all five masses in the same manner as it was computed for the pump dependence. In general, for each of the five masses, the probe intensity dependence shows a mirror image of the behavior of the pump dependence. For the probe dependence, the slope starts off high and then immediately decays to a lower value. The HgI, I, and Hg slope plots resemble one another. For these three masses, the slope of the probe dependence initially decreases from a value of about 1.5 to a minimum at around 500 fs, and it then increases at longer times. For HgI_2, on the other hand, the slope keeps decreasing at long times, and for I_2 there is severe probe saturation at long times as indicated by the fact that the slope approaches zero.
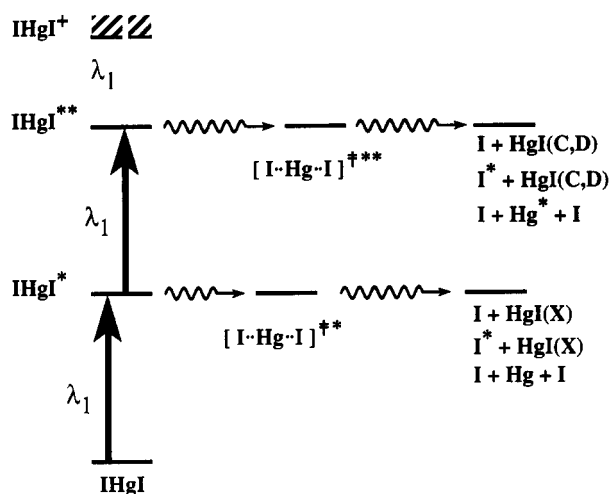
Figure 7. A schematic for the different channels involved in the fragmentation by one photon and multiphoton excitations (see text).

IV. Discussion

From the results of the pump dependence slope plots, it is clear that there is a one-photon excitation process as well as a two-photon process. Three pump photons have sufficient energy to ionize the system, but in the experiment, the MPI background HgI_2 ion signal due to the pump only was reduced to a negligible level.

Consider first the one-pump-photon excitation process (for absorption spectrum see ref 7). This process was detailed in ref 7 and is summarized as follows: After the excitation, the system evolves on the order of 50 fs into the transition state. This explains the time shifts in the rise of the fragment transients with respect to HgI_2. In the transition state, the probing wavelength (622 nm) is resonant (or nearly so), while for the final HgI fragment it is off-resonant (see Figure 9 of ref 2). We observed a double structure on HgI, I, and Hg due to the different fragmentation channels that lead to the final products: $I + HgI(X)$, $I^* + HgI(X)$, $I + Hg + I$ (see Figure 7 and ref 7). The transition state, leading to $I + HgI(X)$, is entered at about 50 fs, while the transition state corresponding to the channel with final products, $I^* + HgI(X)$, is entered at approximately 270 fs, since a separation of about 220 fs is observed for the two peaks in the HgI transient. HgI originates through an asymmetric stretch, while the I fragment can result from either a symmetric stretch or an asymmetric stretch channel, as discussed in ref 7. The first peak in the Hg transient is attributed to the symmetric stretch motion.

As in the detection of fluorescence from HgI,[1-4] the same double structure was seen here, detecting the HgI ion mass. Both types of experiments yield information on how long the system remains in the transition state. The system, upon leaving the transition state, can no longer be excited to the B state, and hence no fluorescence of HgI was seen after this time of ~500 fs.

Any signal due to the free fragments from a one-pump-photon excitation must be due to MPI nonresonant transitions (4 + 2 for both Hg and I; 4 + 1 for I*; first step is nonresonant for HgI). Any MPI signal, if present, from these final free fragments will result in a small constant background after approximately 500 fs.

Let us turn to the two-pump-photon excitation process. All transients show a pump power dependence with a slope that at very early times is approximately equal to 1 but then rises to a constant asymptotic value that lies in the range 1.8 ± 0.3. An on-resonant two-photon transition (with sufficiently long lifetime) should have a slope near 1, and an off-resonant two-photon transition would result in a slope of 2. The first pump photon excitation ($HgI_2 \rightarrow HgI_2^*$, see Figure 7) is resonant, as a broad absorption feature exists for this transition (see ref 7). The first

excited state decays very fast (~50 fs), so that absorption of a second pump photon during this decay period can explain our partly off-resonance behavior in the slope for the two-photon excitation process. From this we conclude that, for every mass, a one-photon pump excitation process is dominant only in the early time regime, giving rise to fast dynamics on the first excited potential energy surface, while a two-photon pump excitation leads to a type of dynamics that dominates and persists at long times.

The time for the rise in the pump dependence slope from a value very near 1 to the asymptotic permanent value of about 1.8 is not the same for all masses. For HgI, Hg, and I, however, this rise time is almost identical (approximately 400 fs). The rise time in the slope for HgI_2 is about 200 fs, which reflects that the decay time away from the one-pump-photon excited initial region of the potential energy surface must be less than 200 fs, consistent with the initial very fast decay time in the HgI_2 transient (Figure 1). (From simulations, the cross-correlation of the pulses broadens the rise time in the slope plot.) Finally, in the case of I_2, the rise for the slope starts at a time delay of about 100 fs and is completed less than 100 fs later. This behavior can be explained as follows: the probe accesses the ion from the one-photon pump excited surface by MPI, causing a slope of 1 in the pump dependence in the first 100 fs. Within the pump pulse duration, the system evolves on the first excited state before a second pump photon further excites the system to the second excited level, which can be probed on a long time scale.

We now consider the long-time behavior. In both of the transients for HgI and I, we see a buildup (bump) in the signal on a time scale on the order of 1 ps, followed by a decay in less than 10 ps to an asymptotic value as discussed before in the Results section (see Figures 2, 3, and 6). This behavior can be explained by an evolution of the system through a transition state to final products. Note that this long buildup time (~1 ps) is not typical of a direct fragmentation but more likely due to an initially excited quasi-bound state in the parent molecule that is crossed by surfaces leading to the final products. The HgI production is promoted by an asymmetric stretch, while the Hg is most probably due to a symmetric stretch mode. For HgI and I, the decay of the transition state reflects the decay in the transient to its asymptotic value which is constant up to 100 ps (limit of experimental range).

Energetically, the B, C, and D states of HgI are accessible as final products. (The B state would be accessed above its dissociation limit, however). These are electronically excited states and hence give rise to a resonant MPI process. This explains the high asymptotic signal level for HgI as resulting from ionization of the electronically excited free fragments. Note that the fluorescence lifetime of these states is on the nanosecond time scale. For example, the B-state lifetime is 23 ± 1 ns.[9]

The I fragment is produced in its ground state ($^2I_{3/2}$) or its spin–orbit excited state ($^2I_{1/2}$), and using the same argument as for the final products formed from one-pump-photon excitation, the off-resonant MPI could contribute to the final value. The pump dependence slope for I at long times is 1.65 ± 0.1, indicating that the contribution to the I signal in the asymptote is due to a two-photon pump process. If the asymptotic signal were due to nonresonant probing (4 + 1 for I*, 4 + 2 for I), then we would have expected more contribution from the one-pump-photon excitation process because it should have a higher yield of free I and I*. This would, in turn, have implied a pump dependence slope of 1 for the asymptotic I signal. We see a steeper slope (1.65 ± 0.1), and hence we must explain the asymptotic I signal by another means. We attribute it to a probe ionization of the electronically excited HgI (that resulted from a two-photon pump process), followed by ionic fragmentation due to further absorption of probe photons. This argument is supported by the following observations. The HgI and I transients show the same long-time

behavior; they both have appreciable signal after 500 fs, which is followed by a decrease in less than 10 ps to an asymptotic constant signal level. The pump dependence slope plot for HgI resembles that for I, and the probe dependence slope plots for the two masses are also very similar in their dynamical features.

The probe dependence slope decreases for HgI and I to a minimum at about 500 fs, followed by an increase in the slope. The decrease reflects a growing contribution to the signal from the transition state of the two-pump-photon excited surface. The increase that follows indicates that the probing cross section decreases upon leaving the transition state and reaching the final products. (For fixed pulse intensity and wavelength, saturation will only depend on the cross section for an excitation.)

The high probe slope in the beginning of the transients does not contradict the fact that the signal is largest at early times. The explanation is that the pump was kept in the unsaturated regime, implying that the one-pump-photon excited surface will be more populated than the two-photon excited surface. Because of the energy difference, the one-pump-photon excited surface requires more probe photons to be ionized, and hence a higher probe dependence slope is associated with the early-time behavior.

The Hg transient is also a superposition of a one- and a two-photon-pump excitation process, as can be seen directly from the pump dependence slope plot (Figure 4). What distinguishes the Hg transient from those of HgI and I is that the Hg transient shows a long time buildup in the signal that persists over tens of picoseconds. We do not attribute this long growth of the Hg signal to be only due to ionic fragmentation of an HgI electronically excited state, as we would then expect a corresponding long-time growth behavior on the I mass. As mentioned earlier, HgI arises from an asymmetric stretch mode, whereas Hg stems from a symmetric stretch mode. If we restrict our discussion to this one-dimensional picture in order to make the general behavior clearer, then this result, the growing of the signal in the transient on a time scale of tens of picoseconds, is analogous to that seen in NaI.[10] It arises from wave packet motion on a bound surface that is crossed by a repulsive surface. Every time the wave packet reaches this crossing region, part of the wave packet leaks out into the asymptote. This behavior is also similar to that of the Rydberg-state dynamics in methyl iodide.[11]

It is the nature of the potentials involved that dictates why buildup of Hg is on the order of tens of picoseconds, whereas the transition-state buildup of HgI is only on the order of 500 fs, and the resulting free fragments of HgI are already formed after less than 10 ps. In order to explain our results, we propose the following: the potential that is reached by a two-pump-photon excitation is bound, but this potential is crossed by two repulsive surfaces accounting for the observed predissociation: (a) One surface has an asymptote to the free HgI(C,D) and I (or I*) products, and the coupling into this surface is promoted by an asymmetric stretch mode. (b) The second surface has an asymptote to the free I + Hg* + I fragments and is coupled to by the symmetric stretch mode.

This second coupling (b) must be weaker than the first one (a) to account for the slow buildup in the Hg channel compared with the fast buildup in the HgI channel. If the initial wave packet were to redistribute quickly into all degrees of freedom, then the parent decay and the product build-up would be dominated by the strongest coupling. As we do see two distinct build-up times on the products, we propose that part of the initial wave packet is not redistributed but rather remains in a defined coordinate leading to symmetric stretch fragmentation with a weak output coupling. So this part of the wave packet is not affected by the strong coupling into the asymmetric stretch coordinate.

The parent decay can now be examined. The different dynamics are reflected in the multiexponential decay of the parent. The one photon pump excitation leads to a fast decay of about 50 fs, as seen in the time shifts of the fragment transients with

respect to time zero of HgI_2. The first component in the multiexponential decay in the HgI_2 transient was also found to be on the order of 50 fs, taking the cross-correlation of the pump and probe into account. Both the pump and probe intensity dependence slopes show a drastic change in the first 200 fs. If we take the cross-correlation into account here, as well as the difference in the cross section between the first and second excited state, then we again arrive at a comparable time constant. The HgI_2 transient was analyzed as a triple-exponential decay (*vide supra*). The first, fast component had $\tau_1 \sim 50$ fs. The longer time components were found to be $\tau_2 \sim 500$ fs and $\tau_3 \sim 1$ ps. Components with even longer decay times could not be extracted due to the low signal-to-noise ratio at long time delays, where the signal dropped toward zero. As the long-time behavior, according to the pump dependence slope plot for HgI_2, is associated with two-photon pump excitation, we attribute the long decay times to the lifetimes of the predissociating bound state.

Finally, we come to I_2 (Figure 5). The pump dependence plot shows a very sharp rise in the slope in less than 100 fs, from an initial value of about 1.2 ± 0.1 to a final constant level of 1.65 ± 0.2. Hence, the dynamics of the I_2 production is governed almost entirely by the two pump photon excitation process. The shape of the I_2 transient, for a given pump and probe intensity, is very similar to the HgI_2 transient. In the discussion so far we have shown that the two-photon excitation involves predissociative states of HgI_2. Because of the long (picosecond) lifetimes of these states, there is enough time for the initial linear IHgI molecule to undergo bending motion. This argument is supported by the relativistic *ab initio* calculations of Wadt[12] on the isoelectronic system $HgCl_2$ which shows bound excited states with an equilibrium angle of 70°–100°. When the bend angle is appreciable, corresponding to a triangular configuration of the molecule in the bound state, I_2 elimination is expected. The probe laser can excite this configuration into an ionic fragmentation channel of HgI_2^+ yielding I_2^+.

The probe dependence slope plot shows that initially the I_2 signal has a slope of 0.6 ± 0.2, reflecting some saturation, but this dependence changes to severe saturation at 200 fs (earlier when convolution with cross-correlation is considered). The probe dependence behavior mirrors that of the pump dependence. Thus, the probing transition of I_2, out of the two-pump-photon excited bound state, is a saturated transition, at the probe intensities used. Note that saturation affects transients over a time range of the order of the width of the cross-correlation only, and hence the long-time decay components are relatively unaffected. Saturation also affects the degree of polarization anisotropy, as discussed in ref 7.

V. Summary and Conclusions

Real-time studies of the HgI_2 reaction in a molecular beam are reported here. The reaction was initiated by a femtosecond laser pulse at 311 nm and followed by a time delayed probe laser (622 nm) which ionizes the parent molecule, the reaction intermediates, and final fragments by REMPI processes. Transients were obtained for all masses (HgI_2^+, HgI^+, I_2^+, Hg^+, and I^+), and careful pump and probe intensity dependence studies were performed on each mass. The method of obtaining the slope of the intensity dependence as a function of the pump–probe time delay provides the means of tracking and distinguishing between one-photon or multiphoton excitations, the onset and presence of saturation, and the time scales associated with different dynamical processes.

In the preceding paper,[7] the dynamics on the dissociative A-continuum reached by one-photon excitation were detailed. Here, the two-photon excitation accesses predissociative states of HgI_2, with crossings into the symmetric and asymmetric stretch coordinates. The transition states and the resulting free fragments ($HgI(C,D)$ and Hg^*) were probed on the time scale of these

experiments. The analogy with Rydberg-state dynamics is discussed. The time scale for all coordinates, including the bend motion, are the key to final fragmentations into different nascent products (HgI, I, Hg, I_2). Further studies are planned with focus on ionic fragmentation, molecular dynamics simulations, and energy dependences of the observed rates of fragmentation and elimination.

References and Notes

(1) Bowman, R. M.; Dantus, M.; Zewail, A. H. *Chem. Phys. Lett.* **1989**, *161*, 297.

(2) Dantus, M.; Bowman, R. M.; Gruebele, M.; Zewail, A. H. *J. Chem. Phys.* **1989**, *91*, 7437.

(3) Gruebele, M.; Roberts, G.; Zewail, A. H. *Philos. Trans R. Soc. London, A* **1990**, *332*, 223.

(4) Zewail, A. H. *Faraday Discuss. Chem. Soc.* **1991**, *91*, 207.

(5) McGarvey, J. A., Jr.; Cheung, N. H.; Erlandson, A. C.; Cool, T. A. *J. Chem. Phys.* **1981**, *74*, 5133.

(6) Cheung, N. H.; Cool, T. A. *J. Quantum Spectrosc. Radiat. Transfer* **1979**, *21*, 397.

(7) Baumert, T.; Pedersen, S.; Zewail, A. H. *J. Phys. Chem.*, preceding paper in this issue.

(8) Rosker, M. J.; Dantus, M.; Zewail, A. H. *J. Chem. Phys.* **1988**, *89*, 6113.

(9) Whitehurst, C.; King, T. A. *J. Phys. B: At. Mol. Phys.* **1987**, *20*, 4035.

(10) Rose, T. S.; Rosker, M. J.; Zewail, A. H. *J. Chem. Phys.* **1989**, *91*, 7415

(11) Janssen, M. H. M.; Dantus, M.; Guo, H.; Zewail, A. H. *Chem. Phys. Lett.*, in press.

(12) Wadt, W. R. *J. Chem. Phys.* **1980**, *72*, 2469.